

MECHANISMS FOR CARBON MIGRATION AND DEUTERIUM RETENTION IN TORE SUPRA CIEL LONG DISCHARGES

J.T. Hogan¹, E. Dufour², P. Monier-Garbet², C. Lowry³, Y. Corre²,
 J. Gunn², R. Mitteau², E. Tsitrone², C. Brosset², J. Bucalossi², T. Loarer²,
 I. Nanobashvili², B. Pégourié², P. Thomas² and the Tore Supra Team

¹ : Fusion Energy Division, ORNL, Oak Ridge, TN 37831-8072 USA

² ; Association Euratom-CEA, CEA Cadarache, CEA-DSM-DRFC, F-13108 Saint Paul-lez-Durance, France

³ ; ITER Joint Work Site, Cadarache, F-13108 Saint Paul-lez-Durance, France

E-mail contact of main author: hoganjt@ornl.gov

Abstract: A model has been created to examine, in greater detail, co-deposition mechanisms in Tore Supra long discharges with high extracted power. The model couples 1D core, 3D scrape-off layer and detailed 3D wall impurity generation models to follow the C balance in steady state. It describes the complex 3D erosion/deposition zones of the Tore Supra CIEL surface, and includes a description of impurity generation from intra-tile gaps and from the poorly adhered layers of re-deposited material in shadowed areas. Results have been compared with CII/D_a spectroscopy for a power scan in a database of 50 discharges. The model reproduces the observed increase in CII emission with power. Sources due to D⁺ physical sputtering are found to saturate at higher net power levels, while self-sputtering contributions continue to increase. A new mechanism for transport of deposited C to remote areas is suggested from the model: radiant heating of poorly adhered layers, combined with CX bombardment, can cause layer decomposition and further transport. This is relevant to the resolution of questions concerning the observation of large scale deposits (flakes) in areas on JET and in other devices. A scaling for the dependence of total carbon erosion on plasma parameters has been inferred from the spectroscopic database, and used to make a shot-by-shot analysis of 3 sequential Tore Supra annual campaigns in order to establish a direct relation between spectroscopic observation and total erosion..

1 Introduction

A study of carbon generation and related co-deposition in long Tore Supra CIEL discharges has been undertaken because of the importance of such processes to predicting tritium retention and diagnostic mirror coating rates for ITER. However, more fundamentally, CIEL experiments with all-carbon plasma-facing components have produced a complex environment of eroded and re-deposited zones, of material deposited in intra-tile gaps, and of re-deposited layers with poor thermal connection to the active cooling system. The overall pattern is established by the rippled magnetic field geometry and its accompanying self-shadowing effects. Since such complex features will also be produced by ITER steady state operation with carbon-based plasma-facing components, this complex environment, rather than the spatially homogeneous idealizations now studied, should be considered in studies of ITER tritium retention and mirror coating rates, and in making steady state performance estimates.

The elements of this study are a quantitative database of measured CII and D_a emission from selected zones on the toroidal pumped limiter (TPL) of CIEL [1], and a model which couples wall generation, SOL and core transport processes to provide a comparison with the spectroscopic observations. The characteristics of the experimental database are described in section 2. The coupled model has been previously described [2, 3], and only pertinent aspects for the complex CIEL environment, including the proposal for a novel radiative impurity generation and transport effect, are presented in section 3. Experimental data consistency comparisons are described in section 4. The comparison of model and

database is described, and a scaling relation between carbon production and plasma parameters is deduced from the experimental database in section 5. Using the resulting scaling law, a shot-by-shot analysis of Tore Supra CIEL campaigns 2002-2003-2004 has been made and results for cumulative C erosion are presented in section 6. Section 7 is devoted to conclusions and discussion.

2 Experimental database

2.1 Long discharge scenario and plasma edge parameters

The long discharges studied in this work use a plasma scenario ($I_p = 0.6$ MA, $B_t = 3.8$ T, $V_{loop} \sim 0$) sustained by lower hybrid current drive alone or by combined lower hybrid current drive and ion cyclotron heating ($0 < P_{LH} < 4$ MW, $0 < P_{ICRH} < 2.5$ MW), with a line integrated density nl varying from 1.4 to 5.2×10^{19} m⁻². A few ohmic discharges with the same global parameters but shorter pulse duration are also studied. The corresponding plasma edge parameters are measured by a reciprocating Langmuir probe located on the top of the torus. The edge electron density n_e^{edge} at the last closed flux surface (LCFS) varies from 1.0×10^{18} m⁻³ for ohmic discharges to 1.1×10^{19} m⁻³ for combined power discharges, while the edge electron temperature T_e^{edge} at the LCFS varies from 15 (in Ohmic discharges) to 45 eV.

2.1 Local carbon flux measurement

The main diagnostic used for evaluating carbon fluxes from the TPL is a visible telescope, located on top of the torus, allowing a direct view of the TPL. This diagnostic comprises a CCD camera with interchangeable interference filters and four optical fibres connected to a visible Czerny-Turner spectrometer, which observes CII (658.1 nm) and D_α (656.3 nm) spectral lines. For this study we use one of the four fibres, located in a net erosion zone (plasma interaction area). Local values of edge density and temperature for this fibre are taken at the LCFS. Atomic carbon fluxes $\Gamma_{C_0}^{in}$ from the TPL surface are deduced from the CII spectral line brightness, calculating the S/XB ratio from local edge parameters. (S and X are the ionisation and excitation rate coefficients, and B is the branching ratio).

2.3 experimental data consistency

The consistency of Langmuir probe measurements with other plasma data is important both for the experimental interpretation, in the calculation of S/XB ratios, and because modelling which relies on these edge data is used to calculate total eroded fluxes from the local fibre measurement. Consistency has been verified by comparing the net conducted power ($P_{input} - P_{rad}$) with power deduced from Langmuir probe data for $n_e^{edge} \times T_e^{edge 3/2}$ for shots in the database. We have also compared the deuterium flux deduced from D_α spectroscopy (656.3 nm) with the deuterium flux calculated from Langmuir probe data, corrected for carbon fluxes incident on the probe and this also demonstrates good consistency of the spectroscopy measurements with the probe data.

3. Coupled model for erosion

3.1 Model elements

A coupled codes model, described in [2], is applied to describe carbon generation and transport in and through the SOL, and impurity transport in the core. The codes IMPFLU, BBQ, and ITC/MIST are used in an iterative fashion to calculate the C balance. IMPFLU is an adaptation of the TOKAFLU module of CAST3M, a 3-D, time-dependent finite elements code which determines the thermal properties of plasma-facing components in the actively mcooled CIEL system. IMPFLU calculates the spatial distribution of C sputtering fluxes and

the emergent energy distributions on the face of the TPL as input to SOL Monte Carlo transport calculations. BBQ is a Monte Carlo guiding center code which describes trace impurity transport in a 3-D defined-plasma background, to calculate line emission for comparison with spectroscopy and to provide poloidally varying boundary conditions for core transport; ITC and MIST are radial core multi-species impurity transport codes which provide the efflux from the core for self-sputtering estimates. Further descriptions of both the component codes and the coupled system are given in [2].

3.2 Modeling the CIEL environment

The evolution of the CIEL environment with the progress of long discharge operation has been described in [4]. Thick carbonaceous deposits appear over 100s of discharges in shadowed areas, along with continuous growth in deposits of material in intra-gap regions. Thus, modifications to idealized CIEL models are required to account for sources from deposited layers and from intra-tile gaps. As shown in [4], intra-tile gap regions in the

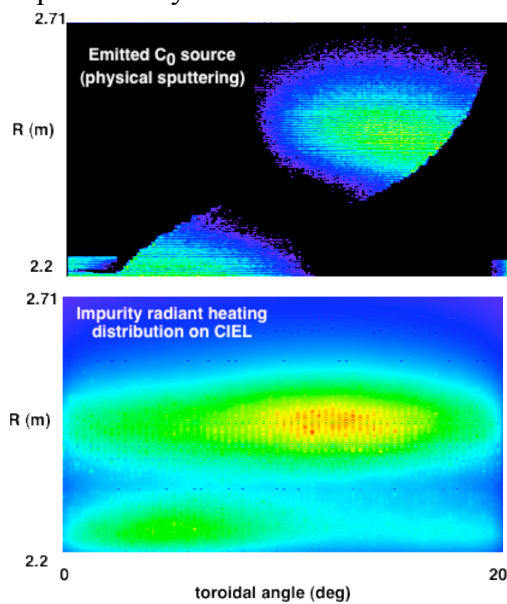


Figure 1. BBQ comparison of C emission from erosion zones (top) and resulting distribution of radiant flux incident on CIEL from impurity radiation.

convected zone gradually show higher temperatures over many discharges, possibly due to the deposition of material in these gaps. To account for this, the BBQ model for carbon generation rates is modified by using the experimentally measured (IR) values for local temperature for the gap regions. We assume that the gaps are filled with deposited material, and no explicit account is taken of possible leading edge heating. Further data consistency simulations, carried out to assess the degree to which local spectroscopic measurements reflect local generation processes, are described in [3].

3.3 Radiative impurity generation and transport mechanism

Infra-red maps of temperature on the TPL [4] outline the regions of thick deposits in shadowed areas with locally high surface temperature. While the shadowed areas are not exposed to directly convected flux in the

deposition region, impurity generation can be expected from these zones if we account for the heating of such $\sim 10\text{-}50\mu\text{m}$ layers due to radiation from impurities produced only in the convective zones. For a nominal higher power case, and $P_{\text{rad}} = 0.4 P_{\text{in}}$, idealized estimates of radiative heating, assuming that the radiation is localized on the tokamak plasma magnetic axis, yield a radiant heat flux of 0.03 MW/m^2 , compared with $\sim 2\text{-}3 \text{ MW/m}^2$ convected flux. Several non-ideal factors serve to modify this picture : 1) the impurity radiation due to convective zone impurities is localized near the TPL, so the radiation view-factor is $\sim 50\%$, rather than 15% in the case of axis localization, the based on the intercepted solid angle ; 2), 3) impurity radiation is both poloidally and toroidally localized due to the ripple, providing a $\sim 9\text{-fold}$ increase over the idealized (uniformly distributed) case. These combined enhancement factors produce a peak ambient radiant flux of $\sim 0.3 \text{ MW/m}^2$, falling on the shadowed regions of the TPL. The radiant density on the TPL is calculated using BBQ from a 5 dimensional integral, in which the radiation flux from each zone of the 3-D impurity radiated power distribution is calculated for each point on the 2D TPL surface. The radiant

flux profile is found to be more widely distributed than either the impurity density or radiation profile, as shown in Figure 1, and can thus be a significant source of heating for layers in the shadowed regions [5]. These deposited layers are thermally isolated from the actively cooled CIEL system and reach peak values for shadowed areas (as found from IR measurement) from 400K – 1100K as P_{in} varies from 1 – 3 MW. Such temperatures are optimal for chemical erosion, but they are found in shadowed areas, where the direct ion flux is small. Previous Eirene calculations [6], however, indicate that neutral charge exchange flux to the TPL amounts to $\sim 30\%$ of the incident convective flux. The CX bombardment is dispersed similarly to the radiant flux, and so the generation pattern for chemical erosion due to CX is expected to be broad also and this can be a significant erosion mechanism.

4. Experimental scaling of carbon local fluxes

4.1 Comparison with data

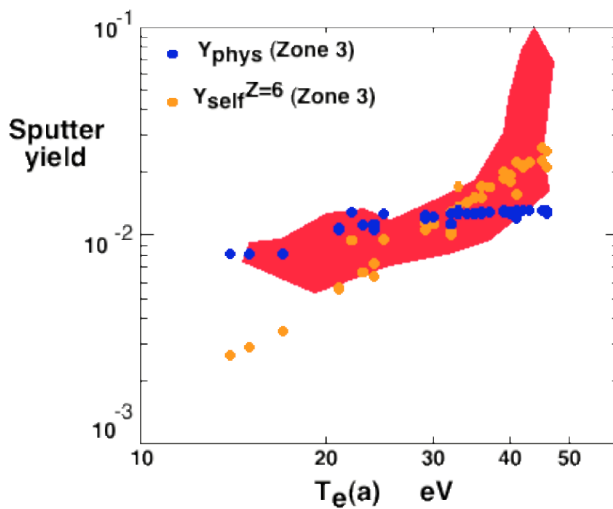


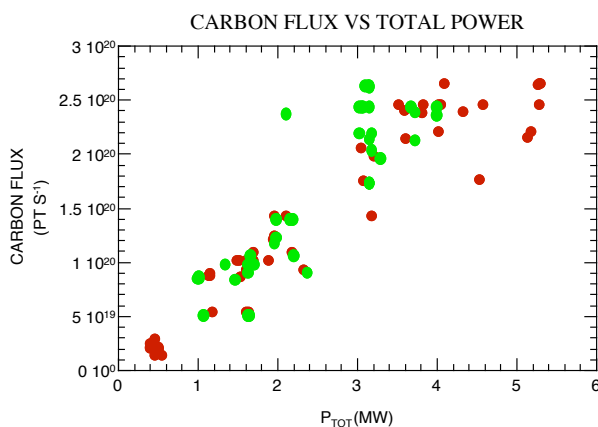
Figure 2. Comparison of BBQ calculations for physical and self-sputtering yields with values from spectroscopic database

We use the experimental ratios of carbon fluxes, obtained using the S/XB method to give an empirical estimate of the total sputtering yield integrated over the fibre spot size. This value is compared with the IMPFLU/BBQ values for the same quantity, as calculated with the procedure described in section 2. The comparison is shown in Figure 2. The solid color (red) area is the region of measured values. For comparison the model values for the same quantity are shown, for physical and self-sputtering processes. The self-sputtering values (“ Y_{self} ”) are defined

as the ratio of self-sputtered carbon flux to D^+ influx, rather than the actual self-sputtering yield for C^{n+} impact. The model values are calculated with the edge plasma

data and magnetic configuration for each of the shots, and the measured Z_{eff} for that shot is used to calculate the carbon efflux which is used to calculate self-sputtering. The charge state distributions of the carbon efflux are found from MIST radial transport calculations and expressed as a fraction of the D^+ ion efflux in order to calculate the equivalent “ Y_{self} ”.

4.3 Experimental scaling of C fluxes



The particle fluxes based on CII brightnesses are shown on Figure 3 for shots from the experimental database for fibre 3. We have used modelling to estimate the ratio of the total carbon production from the TPL to the production measured from this fibre. The BBQ code has been used to

Figure 3 CII flux vs total power for shots with LH (green) and with LH power and additional RF heating (red)

determine the ratio of the C production measured by fibre 3 to the total for all the fibres for a sample set of cases from the database. The ratio of the flux from the fibre to the total flux integrated over one of the 18 modules of CIEL, uses results for physical and self-sputtering processes since these are dominant in the high power regime. Both ratios are found to be approximately constant with variations in convected power and so we use a multiplication factor of 8 to relate the fibre 3 values to the total flux for one CIEL module. The CII flux density increases approximately linearly with P_{LH} , but does not further increase with additional RF power. Thus the scaling relation used for cumulative erosion estimates for one fibre is $\Gamma_{CII} \text{ (pt/m}^2\text{/s)} = 0.62 \cdot 10^{20} P_{conv} \text{ (MW)}$, where P_{cond} is the conducted power ($P_{ohmic} + P_{LH} + P_{ICRH} - P_{rad}$). For the total C generation it is $\Phi_C \text{ (pt/s)} = 5 \cdot 10^{20} P_{conv} \text{ (MW)}$,

5 Carbon erosion over three annual campaigns

Using the spectroscopic database we have constructed an estimate of the amount of C spectroscopically observed to be removed. Such observations may present an overestimate since in principle eroded carbon could be re-deposited and then observed to be subsequently re-eroded. But the largest fluxes dominate the overall C balance, and these arise from net erosion zones, so the total obtained is thought to be in the proper scale.

5.1 Conditions over the campaigns

The 2002-2004 Tore Supra campaigns were devoted to high power, long discharges. Of ~ 4011 successful discharges, 1375 used Lower Hybrid injection alone and 922 also used RF power. The plasma current for the pulses was distributed as 29% with $I_p < 0.7$ MA, 71% with $0.7 < I_p < 1.1$ MA and 20% with $I_p > 1.1$ MA

5.2 Cumulative carbon erosion 2002-2004

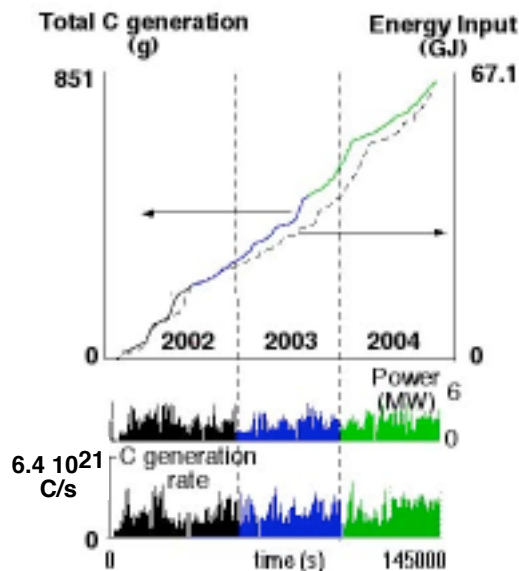


Figure 4. Instantaneous power and C generation rate (bottom) accumulated injected energy and cumulative eroded C for each shot in the 2002-2004 campaign, from spectroscopic scaling.

The total injected energy is shown, from a shot-by-shot analysis, in Fig. [4]. A total of ~ 67 GJ was extracted by CIEL during this period. We have applied the scaling law described in section 4 to the time sequence of each discharge in the 2003-2004 campaigns. For the campaigns considered, comprising about 2400 discharges, with ohmic, LH and LH+ICRH operation, and a mixture of pulse lengths, the instantaneous C generation rate was calculated for all times during each discharge, and the total C generation was accumulated by integrating this rate. For fewer than 10% of the discharges, the radiated power data were not available and in such cases we estimated that $P_{rad} = 0.4 P_{inj}$.

Figure 4 also shows the instantaneous C production rate during each of the discharges, and the estimated accumulated C production over the 2002-2004 campaigns. In an accumulated total of 145000 s of plasma operation, 851 g of carbon was deduced to be removed, according

the spectroscopic scaling deduced from fibre 3 measurement and BBQ modeling.

For comparison, after one campaign ~ 1.5 g carbon deposits were scraped from localized regions on the outboard movable limiter, ~ 5.5 g from one section of the TPL, ~ 1 g from LH launchers and ICRH antennas, and ~ 10 g from neutralizers [7]. Additional C remains in the machine in volumes under the TPL and below the tiles of the inner bumpers. Assuming similar values for 2002-2004, then, ~ 40 g of carbon deposits have been identified for these campaigns, i.e. between 15 and 30 g per campaign. If we compare the eroded carbon quantity estimated from spectroscopy with that collected, we can see that only a small amount of the estimated eroded carbon has been accounted for in the machine.

It is estimated that $8 \cdot 10^{23}$ D atoms were permanently retained from the 2004 campaign [7]. Using this figure as typical also for 2002 and 2003, we arrive at $2.4 \cdot 10^{24}$ D atoms retained; in respect to the estimated carbon removal, this is a ratio of ~ 0.05 - 0.1 D/C for the 2002-2004 period.

6. Discussion and conclusions

A comparison of model values for the ratio of C and D fluxes with the equivalent experimental values shows reasonable agreement. The scaling for physical sputtering alone saturates with increasing $T_{e, \text{edge}}$ in this database; however contributions from self-sputtering become dominant in the high edge temperature region and the overall agreement is good. Model cases at the highest values of $T_{e, \text{edge}}$, where self-sputtering is most important, show somewhat lower values, but the higher experimental values are cases with $Z_{\text{eff}} > 3$ and have not been analyzed yet. The results also bear on the prediction of diagnostic mirror coating rates for ITER. A study is in progress to compare the C removal and co-deposition rates over the 2002-2004 campaign of high power, long discharges in Tore Supra using the spectroscopy-based analysis. The model also shows that impurities generated in the convective zone produce local radiant heating of layers in shadowed zones. Although such erosion from shadowed zones is not a significant contributor to the instantaneous fluxes in this comparison, it may serve as a long term mechanism to move deposited carbon from shadowed to remote areas. This mechanism may also be operative in axi-symmetric divertors, since a strong localized radiation source exists at the x-point, and deposited layers are found outside the divertor strike points, which are also a source of potentially large charge exchange fluxes to the nearby radiantly heated deposited layers. Thus this mechanism provides a possible means to move deposited carbon to more remote regions such as louvres or pump ducts which are not directly illuminated by convective flux.

Acknowledgement: ORNL sponsored by Oak Ridge National Laboratory managed by UT-Battelle, LLC, for the U.S. Department of Energy under contract DE-AC05-00OR22725

References

- [1] E. Dufour, C. Brosset, C. Lowry, Proceedings of the 32nd European Physical Society Conference, Tarragona, Spain, 2005
- [2] J. Hogan et al, Contrib. Plasma Physics, **46** (2006) 273
- [3] R. Mitteau, D. Guilhem, R. Reichle et al, Nucl. Fusion **46** (2006) 549
- [4] Y. Corre et al, Proceedings of the 32nd EPS Conference, Tarragona, Spain, 2005
- [5] J Hogan et al, submitted Jour Nucl Mater, PSI-17 Hefei China 2006
- [6] E Tsitrone et al, 20th IAEA Fusion Energy Conference, Vilamoura, Portugal (2004)
- [7] E Tsitrone et al J. Nucl. Mater. **337** (2005) 539